Colloid Polym Sci 275:1035–1045 (1997)

ORIGINAL CONTRIBUTION

E. Piorkowska

Nonisothermal crystallization of polymers in samples of finite dimensions

1. Background of the mathematical description of spherulitic pattern formation

Received: 5 August 1996
Accepted: 17 July 1997

Dr. E. Piorkowska (✉)
Centre of Molecular and
Macromolecular Studies
Polish Academy of Sciences
Siekiewicza 112
90-363 Lodz, Poland

Abstract The mathematical description of the kinetics of spherulitic patterns formation during isothermal and nonisothermal crystallization in samples of finite thickness, strips and plates, is based on the assumption of the momentary randomness of primary nucleation. The time distributions of the formation of the spherulite interiors as well as the time dependence of the conversion degree of a melt into spherulites are derived for time dependent primary nucleation rate and spherulite growth rate. The spherulitic final pattern is described by means of the distributions of distances from spherulite centers to spherulite internal points. The influence of the nucleation of sample boundaries on the kinetics of crystallization and on the final spherulitic structure is also determined. In all dependencies derived the components resulting from both nucleation processes – at sample boundaries and inside a sample – are distinguished.

Key words Nonisothermal crystallization – confined samples – conversion degree

Introduction

The first attempts to describe the formation of structure of crystalline domains growing from random nuclei were focussed on the kinetics of that process, i.e., on the description of conversion of melt into domains [1–3]. Kolmogoroff and Evans calculated the probability that an arbitrarily chosen points remain unoccluded by spheres or circles expanding from nuclei distributed randomly in the sample. Avrami introduced the concept of the so-called "extended volume", E, the total volume of all domains growing from all nuclei including "phantom" domains expanding from nucleation events in the already crystallized area and neglecting the truncation. Thus, the conversion degree at a certain time is expressed by the well known equation:

$$\alpha(t) = 1 - \exp[-E(t)] , \quad (1)$$

where E denotes the "extended volume" or "expectancy". All three approaches are equivalent and based on the same assumption: only the first expanding spheres or circles arriving at a sample point are real still growing domains; "phantoms" and domains excluded from further growth due to truncation with neighbors are always delayed. The Evans approach was also applied by Billon et al. [4] to obtain the expectancy for time dependent nucleation rate and earlier by Ozawa [5] for the problem of the temperature dependent nucleation and growth rate with additional assumption that the temperature changes linearly with time. However, the expressions for $E(t)$ for infinite samples and the same nucleation and growth rate time dependencies derived according to either Avrami or Evans approaches although having apparent different mathematical forms, are equivalent. This can be proved by performing simple integration by parts of the respective expressions in refs. [4, 5].

Colloid & Polymer Science, Vol. 275, No. 11 (1997)

While the results of computer simulation of spherulitic crystallization [6, 7] were in very good agreement with the Avrami theory, many authors pointed out the reasons of discrepancies between the theoretically predicted value of the Avrami exponent and the experimental data [6–11].

Avrami elaborated also a general approach to the problem of conversion of melt into spherulites [3] indicating that the "extended" volume $E(t, A)$ around a certain point of a sample, A, is equivalent to the average number of extended domains which occluded the point A, hence: it is the integral of nucleation rate, F, depending on time τ and position in a sample, over time and over the so-called "region of influence of A":

$$E(t, A) = \int_0^{\pi} \int_0^{2\pi} \int_0^{R} \left[\int_0^{t'} F(\tau, r, \theta, \varphi)\, d\tau \right] r^2 \sin\theta\, dr\, d\varphi\, d\theta , \qquad (2)$$

where r, θ, φ are spherical coordinates originating at A, t' denotes the nucleation time for the domain nucleated at the position (r, θ, φ) and reaching the point A exactly at time t. Time t' must be found from the differential equation $d\rho = -G(\tau, r, \theta, \varphi)\, d\tau$ fulfilling the conditions: $\tau = t$ at $\rho = 0$ and $\tau = t'$ at $\rho = r$, where G denotes the growth rate of domains dependent on time and position. $R(\theta, \varphi, t)$ denotes the radius at time t of the domain nucleated at time $t' = 0$ at θ, φ and reaching the point A at time t: $R = r$ for $t' = 0$. Although Eq. (2) permits to describe the kinetics of crystallization in complicated conditions, e.g. in the presence of temperature gradients no such applications of that formula were demonstrated so far.

Piorkowska and Galeski [12, 13] and Piorkowska [14–16] have developed a method which enables one to evaluate not only the conversion degree of melt into domains but also to describe the domain structure during the formation process and the final pattern of spherulitic structure. The method is based on the concept of nucleation attempts as random events in space and time. It was demonstrated that the method could be applied to the description of both isothermal and nonisothermal processes. The way of calculating the conversion degree for any dependence of nucleation rate and spherulite growth rate on time and position was shown in ref. [12], leading of course to Eq. (2). It was suggested that the assumption of zero nucleation rate beyond boundaries of the material directly leads to dependencies for confined volumes. The expressions for the dependence of the conversion degree on time derived for the nucleation rate and spherulite growth rate dependent on time only [12–14] lead to those obtained earlier [1–4]. However, the approach presented in refs. [12–16], unlike any other, allows to describe not only the conversion of melt into spherulites but also the evolution of spherulites interiors and boundaries and to characterize the final spherulitic structure. The assumption of randomness of nucleation process also in time is very realistic since new nuclei do not appear at uniformly equal time intervals. However, it was shown by the author [14] that the expectancies of the process calculated with assumptions of unfluctuated and fluctuated nucleation rate are the same. Hence, in calculations of the conversion degree it leads to the same results as Avrami or Evans approaches. It is expected that similar results can be obtained for the description of the spherulitic structure but no significant advance was achieved so far [17].

The presence of sample boundaries as well as the nucleation on sample surfaces influence the development of spherulitic structure and thus, polymer properties. The effects of finite size and surface nucleation become critical for industrial processes and laboratory measurements (e.g., DSC) where the portions of a polymer bounded by foreign surfaces are crystallized.

Billon et al. [14] and Escleine et al. [18] derived the dependence of conversion degree on the distance from a sample surface in a plate bounded by two parallel planes for isothermal conditions by calculating the Avrami "extended volume" and the Evans "expectancy" for such case. They pointed out that the finite sample thickness may also cause discrepancies between predictions of Avrami and Evans theory for infinite samples and the crystallization of real samples (e.g., in DSC). The conversion degree in the presence of additional nucleation of spherulites at the sample surfaces was also evaluated. Billon and Haudin [19, 20] presented also a generalization of Evans approach, which makes possible to introduce any position and time dependence of nucleation rate and time dependence of spherulite growth rate. The general equation from ref. [20] is equivalent to Eq. (2) except for the fact that the growth rate G does not depend on position, hence t' and R are defined by the relations: $r = \int_{t'}^{t} G(s)\, ds$, $R(t) = \int_0^t G(s)\, ds$. Then, the conversion degree in a plate during nonisothermal crystallization was calculated by representation of nucleation rate position dependence by a Fourier series periodic function [20]. The appropriate setting of the function's parameters permits to establish the nonzero nuleation inside a plate, zero nucleation beyond plate surfaces and to avoid the effects of "parasitic" nuclei introduced by other periods of the function. The numerical calculation have shown that the presence of boundaries slows down the conversion of melt into spherulites, which can lead to incorrect determination of crystallization kinetics parameters if the data are fitted with Ozawa's equation [5]. It was demonstrated that during cooling the crystallization of polymer at lower temperature could be expected. The nucleation process on sample surfaces was approximated by an additional nucleation process occurring in narrow zones of polymer near the plate's surfaces, characterized by means of supplementary Fourier series

functions [21]. The flat transcrystalline zone growing from a plate surface was also considered. The presented approach allowed to explain the peculiar shape of DSC exotherms recorded during nonisothermal crystallization of polyamide 6-6, with transcrystalline zones growing from sample surfaces. It was concluded, that the beginning of the curve is representative for transcrystallization while the main peak is more sensitive to bulk crystallization. Alternative approach to polymer nonisothermal crystallization in a plate being the direct extension of the theory presented in ref. [4] was also proposed by Piorkowska and Galeski [22].

Recently, the crystallization of a polymer matrix with embedded fibers was investigated by means of a computer simulation [23–25] and also experimentally [26]. It was pointed out that a strong primary nucleation on surfaces of fibers afflicts the kinetics of crystallization. It should be mentioned here that the two-dimensional sample with embedded fibers resembles a sandwich of strips bounded by parallel lines.

Until now all efforts undertaken for the analytical description of crystallization in bounded samples were limited to the conversion of melt into spherulites. Although the importance of nucleation at sample boundaries was emphasized the determination of the conversion degree contributions of spherulites nucleated at sample surfaces and in polymer volume is possible only if intense nucleation process on surfaces results in relatively flat transcrystalline zone, undisturbed by spherulites nucleated in polymer interior.

Below, the rigorous description of the kinetics of spherulitic pattern formation in the vicinity of sample boundaries during crystallization at nonisothermal as well as at isothermal conditions will be presented based on the concept of nucleation as a random process in space and time previously employed by the author for infinite samples [12–16]. The time dependent primary nucleation rate inside the sample and zero nucleation rate beyond sample boundaries will be directly assumed. The influence of nucleation by surfaces of the sample on the spherulitic structure formation will be also evaluated. The nucleation at sample boundaries will be described as the process occurring exactly at surfaces or lines limiting a polymer. This permits to account correctly for the impingement between the spherulites growing from nuclei at sample boundaries (even small displacement of spherulites centers would result in premature truncation of spherulites which were left behind). In order to characterize the final spherulitic pattern the dependencies describing average spherulite radii and distributions of distances from spherulites centers to spherulites inner points will be derived. In all dependencies derived in the paper the two components characterizing both spherulites populations, nucleated inside the polymer and at sample boundaries will be distinguished independently of the intensity of nucleation at material surfaces.

Background of the derivations

The probabilistic approach employed here was previously explained in detail in refs. [14–16]. Hence, only the most important points, necessary for further considerations will be briefly recalled.

1. The considerations that follow are based on the assumption that spherulite nucleation can be described as a set of random attempts occurring in space and in time. Each nucleation attempt creates an expanding circle on a plane or sphere in space but only that attempt which occurs in uncrystallized portion of a sample nucleates a real spherulite. The momentary nucleation rate, $F(t)$, denotes the average number of nucleation attempts per unit time per unit volume and also the number of spherulite centers nucleated per unit time per unit volume of uncrystallized material.

2. At any chosen point of a sample only the first arriving circle or sphere is considered. This permits to exclude from consideration the nucleation attempts occurring in the crystallized fraction of a sample ("phantoms"). Also the real spherulites impeded by others due to truncation will arrive later to the chosen point.

3. Nonisothermal crystallization conditions are accomplished by setting the growth rate, G and momentary nucleation rate, F, dependent on time. Isothermal crystallization is then a particular process with $G = \text{const}$.

4. The expanding circle or sphere nucleated at time τ arises at the point A at a distance r from its nucleation site at time t:

$$r(\tau, t) = \int_{\tau}^{t} G(s)\,\mathrm{d}s \,. \tag{3}$$

Equation (3) defines a circle on a plane or a sphere in space around the point A. For the time interval $(0, t)$, Eq. (3) comprises a curvilinear cone in space and time around a point A having the important property (see Fig. 1 for a plane and time): if n nucleation attempts occur on the surface of that cone then the point A will be occluded at time t simultaneously by n circles (or spheres). If no nucleation attempt occurs inside the cone those circles or spheres will arrive first at point A. Hence, they will represent real spherulites and the point A will constitute the spherulite interior ($n = 1$) or boundary ($n > 1$). For $n = 0$ the point remains unoccluded at time t.

5. The probability of that event, $p_0(t)$, is the probability that no nucleation attempt occurred in successive time intervals $(\tau_i, \tau_i + \mathrm{d}\tau_i)$ until time t inside the space–time

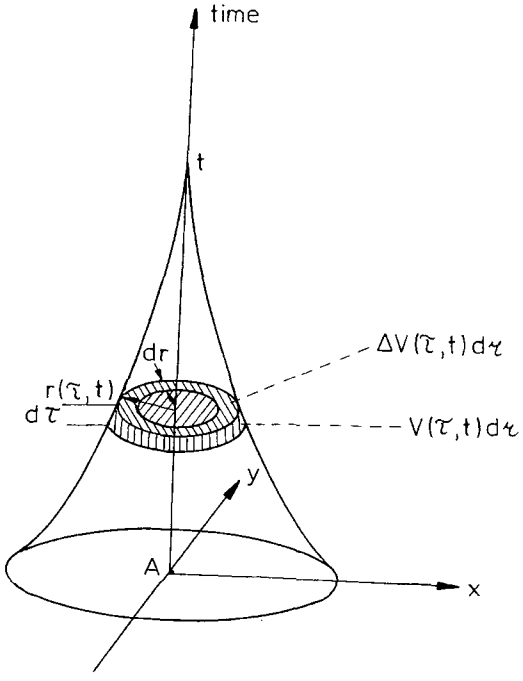

Fig. 1 The cone in a plane – time continuum. The point A denotes the arbitrarily chosen point, $r(\tau, t)$ is the radius of the cone at time τ, $V(\tau, t)\,d\tau$ and $\Delta V(\tau, t)\,d\tau$ are the volume fractions of the cone corresponding to the time interval $(\tau, \tau + d\tau)$ and the volume of the annulus of radius $r(\tau, t)$, respectively

cone around the point A defined by Eq. (3) [14]:

$$p_0(t) = \exp[-E(t)]\,, \tag{4}$$

where $E(t)$ is the integral of $F(\tau)$ over the total volume of the conical zone in space and time:

$$E(t) = \int_0^t F(\tau)\,V(\tau, t)\,d\tau\,, \tag{5}$$

where $V(\tau, t)\,d\tau$ is the volume of that part of the space–time cone which corresponds to the time interval $(\tau, \tau + d\tau)$ (as shown in Fig. 1). For infinite samples:

$$V^{(2)}(\tau, t)\,d\tau = \pi r^2(\tau, t)\,d\tau \tag{6a}$$

$$V^{(3)}(\tau, t)\,d\tau = (4/3)\,\pi r^3(\tau, t)\,d\tau \tag{6b}$$

The numbers in parentheses denote the dimensionality.

6. The probability that the arbitrarily chosen point A is occluded at time t (precisely in time interval $(t, t + dt)$) by one spherulite nucleated at time τ (precisely in time interval $(\tau, \tau + d\tau)$), $p_1(\tau, t)$, is equivalent to the probability that one nucleation attempt occurs at certain time τ within the thin annulus or spherical shell of radius $r(\tau, t)$ and no other nucleation attempts occur inside the space–time cone [12, 14]:

$$p_1(\tau, t) = \exp[-E(t)]\,F(\tau)\,\Delta V(\tau, t)\,d\tau\,, \tag{7}$$

where $\Delta V(\tau, t)\,d\tau$ is the volume of the annulus (Fig. 1) (or spherical shell) of radius $r(\tau, t)$ multiplied by $d\tau$

$$\Delta V(\tau, t) = \frac{dV(\tau, t)}{dr(\tau, t)}\,dr\,, \tag{8}$$

where

$$dr = G(t)\,dt. \tag{9}$$

Below, the time dependence for the conversion degree, the time distributions of the formation of the inner spherulite points and the distributions of distances from spherulite centers to their internal points after completion of crystallization will be derived for samples of finite thickness: a strip and a plate.

Samples bounded by two parallel lines or planes

Let us consider two regions D_1 and D_2 in a sample of infinite volume. A momentary nucleation rate within D_1 and D_2 is different and equal to F_1 and F_2, respectively. In order to calculate the probability that n nucleation attempts occur within the $D_1 + D_2$ we have to summarize all probabilities that k events occur in D_1 and $n - k$ events occur in D_2. Finally we obtain:

$$p_n = \exp(-F_1D_1 - F_2D_2)(F_1D_1 + F_2D_2)^n/n!\,. \tag{10}$$

For samples of finite thickness one has to take into account that there is no nucleation beyond sample boundaries and that at those boundaries an additional nucleation process can occur. Therefore, the summation rule described by Eq. (10) will be applied in further considerations. It should be noted that Eq. (10) for $n = 0$ could be directly obtained from Eq. (2).

Let us consider a sample of thickness $2h$ in x direction and infinite in the directions perpendicular to x-axis; a strip in two dimensions (2D) or a plate in three dimensions (3D). The point A is arbitrarily chosen at distance $d_1 < h$ from the first sample boundary and at distance $d_2 = 2h - d_1$ from the second boundary (Fig. 2). No nucleation occurs beyond sample boundaries. Hence, for the origin of x-axis at the point A:

$$F(\tau) > 0 \quad \text{for } x > -d_1 \text{ and } x < d_2\,, \tag{11a}$$

$$F(\tau) = 0 \quad \text{for } x < -d_1 \text{ and } x > d_2\,. \tag{11b}$$

Usually, samples of finite thickness crystallize between foreign surfaces, hence in many cases the additional nucleation process at sample boundaries occurs. Therefore:

$$F(\tau) = F_s(\tau) \quad \text{for } x = -d_1 \text{ and } x = d_2\,, \tag{11c}$$

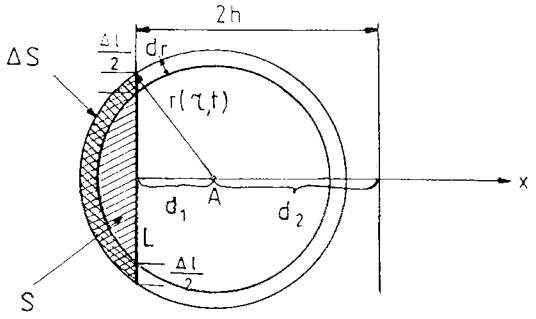

Fig. 2 The position of the point A within a sample. ΔS and S are parts of the circle and the ring of radius $r(\tau, t)$ which are beyond the sample boundary, L and ΔL are parts of sample boundary inside the circle and the ring of radius $r(\tau, t)$

where F_s denotes the number of nucleation attempts per unit time per unit length of boundary line or area of boundary surface. According to Eq. (10) one has to substitute the expressions $F(\tau)V(\tau, t)$ and $F(\tau)\Delta V(\tau, t)$ in Eqs. (5) and (7) with sums of products of $F(\tau)$ and $F_s(\tau)$ by respective volumes in all cases where the space-time cone extends beyond sample boundaries. Hence, Eqs. (5) and (7) have now the following form:

$$E_T(t) = \int_0^t V_T(\tau, t)\,d\tau , \tag{12}$$

$$p_{T1}(\tau, t) = \exp[-E_T(t)]\,\Delta V_T(\tau, t)\,d\tau , \tag{13}$$

where the expressions for $V_T(\tau, t)$ and $\Delta V_T(\tau, t)$ will be derived below.

Let us consider the circle of radii $r(\tau, t)$ and the ring of width dr with the center at the distance d_1 from the sample boundary (Fig. 2). The areas of parts of the circle and ring beyond 2D-sample boundary are expressed as follows:

$$S^{(2)}(\tau, t, d_1) = \gamma(d_1, r(\tau, t))r^2(\tau, t) - d_1[r^2(\tau, t) - d_1^2]^{0.5} , \tag{14a}$$

$$\Delta S^{(2)}(\tau, t, d_1) = 2\gamma(d_1, r(\tau, t))r(\tau, t)\,dr , \tag{14b}$$

$$\text{where } \gamma(d, r(\tau, t)) = \arctan\{[r^2(\tau, t)/d^2 - 1]^{0.5}\} . \tag{15}$$

For 3D-samples the sphere and the spherical shell have to be considered. The volumes of these parts of respective sphere and spherical shell which are outside the sample are described by the equations:

$$S^{(3)}(\tau, t, d_1) = (\pi/3)[d_1^3 + 2r^3(\tau, t) - 3d_1 r^2(\tau, t)] , \tag{16a}$$

$$\Delta S^{(3)}(\tau, t, d_1) = 2\pi r(\tau, t)[r(\tau, t) - d_1]\,dr . \tag{16b}$$

The length of a sector of a boundary line inside a circle of radius $r(\tau, t)$ around the point A (as seen in Fig. 2) is expressed by the equation:

$$L^{(2)}(\tau, t, d_1) = 2[r^2(\tau, t) - d_1^2]^{0.5} . \tag{17a}$$

If a sphere instead of a circle is considered, the area of a boundary plane entering a sphere is

$$L^{(3)}(\tau, t, d_1) = \pi[r^2(\tau, t) - d_1^2] . \tag{17b}$$

The total length of the sectors which are inside a ring of radius $r(\tau, t)$ and width dr, $\Delta L^{(2)}$, and the area of a ring inside the spherical shell of radius $r(\tau, t)$ and of width dr, $\Delta L^{(3)}$, are expressed by the formulas:

$$\Delta L^{(2)}(\tau, t, d_1) = 2r(\tau, t)[r^2(\tau, t) - d_1^2]^{-0.5}\,dr , \tag{18a}$$

$$\Delta L^{(3)}(\tau, t, d_1) = 2\pi r(\tau, t)\,dr . \tag{18b}$$

Hence $V_T(\tau, t)$ and $\Delta V_T(\tau, t)$ can be expressed in the form:

$$V_T(\tau, t) = F(\tau)[V(\tau, t) - S(\tau, t, d_1) - S(\tau, t, d_2)] + F_s(\tau)[L(\tau, t, d_1) + L(\tau, t, d_2)] , \tag{19a}$$

$$\Delta V_T(\tau, t) = F(\tau)[\Delta V(\tau, t) - \Delta S(\tau, t, d_1) - \Delta S(\tau, t, d_2)] + F_s(\tau)[\Delta L(\tau, t, d_1) + \Delta L(\tau, t, d_2)] , \tag{19b}$$

where $S(\tau, t, d)$, $\Delta S(\tau, t, d)$, $L(\tau, t, d)$ and $\Delta L(\tau, t, d)$ have nonzero values if $r(\tau, t) > 0$.

Kinetics of spherulitic structure formation

Below, the expressions for time dependencies of conversion degree and the rate of the formation of spherulite interiors will be derived.

The conversion degree at time t, in a portion of a sample at the distances d_1 and d_2 to sample boundaries, $\alpha(t, d_1, d_2)$, is described by the equation:

$$\alpha(t, d_1, d_2) = 1 - \exp[-E_T(t, d_1, d_2)] \tag{20}$$

where $E_T(t, d_1, d_2)$ according to Eqs. (12) and (19) can be written in the following form:

$$E_T(t, d_1, d_2) = E(t) + H(t, d_1) + H(t, d_2) \tag{21}$$

where the first term, $E(t)$, described by Eqs. (5) and (6), is the integral of nucleation rate $F(\tau)$ over the total conical zone as for infinite samples. The second term, $H(t, d_1)$, and the third term $H(t, d_2)$ are due to the presence of the sample boundaries at the distances d_1 and d_2, respectively:

$$H(t, d) = 0 \quad \text{for } r(0, t) < d , \tag{22a}$$

$$H(t, d) = \int_0^{t^*} [F_s(\tau)L(\tau, t, d) - F(\tau)S(\tau, t, d)]d\tau \quad \text{for } r(0, t) > d , \tag{22b}$$

where L and S are expressed by Eqs. (14a), (16a), (17) and t^* is given by the formula: $r(t^*, t) = d$.

In order to obtain the probability that an arbitrary point is occluded by a spherulite at time t equivalent to the time distribution of formation of spherulite inner points

one has to integrate the probability $p_{T1}(\tau, t)$ expressed by Eq. (13) over the range $0 < \tau < t$:

$$g(t, d_1, d_2)\,dt = \exp[-E_T(t, d_1, d_2)]\,[W(t) + W_1(t, d_1) + W_1(t, d_2)] \,. \quad (23)$$

The term $W(t)$ is the integral of $F(\tau)$ over the entire surface layer of the space–time cone as for an infinite sample:

$$W(t) = \int_0^t F(\tau)\,\Delta V(\tau, t)\,d\tau \,, \quad (24)$$

where ΔV is given by Eq. (8). The terms $W_1(t, d_1)$ and $W_1(t, d_2)$ result from the presence of the sample boundaries at the distances d_1 and d_2 from the considered point A:

$$W_1(t, d) = R_s(t, d) - R_i(t, d) \,, \quad (25)$$

where $R_i(t, d) = 0$ and $R_s(t, d) = 0$ for $r(0, t) < d$,

$$R_s(t, d) = \int_0^{t^*} F_s(\tau)\Delta L(\tau, t, d)\,d\tau \quad \text{for } r(0, t) > d \,, \quad (26a)$$

$$R_i(t, d) = \int_0^{t^*} F(\tau)\Delta S(\tau, t, d)\,d\tau \quad \text{for } r(0, t) > d \,, \quad (26b)$$

where ΔL and ΔS are given by Eqs. (14b), (16b), (18). $g(t, d_1, d_2)$ represents the local rate of conversion of a sample into spherulites at time t in the portion of a material at the distances d_1 and d_2 from sample boundaries. According to Eqs. (25) and (26) $g(t, d_1, d_2)\,dt$ can be expressed as a sum of two components:

$$g(t, d_1, d_2)\,dt = g_i(t, d_1, d_2)\,dt + g_s(t, d_1, d_2)\,dt \,, \quad (27)$$

$$g_i(t, d_1, d_2)\,dt = \exp[-E_T(t, d_1, d_2)][W(t) - R_i(t, d_1) - R_i(t, d_2)] \,, \quad (28)$$

$$g_s(t, d_1, d_2)\,dt = \exp[-E_T(t, d_1, d_2)] \times [R_s(t, d_1) + R_s(t, d_2)] \,, \quad (29)$$

g_i and g_s express the local rates of formation of interiors of spherulites nucleated inside a sample and spherulites nucleated at sample boundaries, respectively. It should be noted that $g_s(t, d_1, d_2)$ assumes nonzero values only if $r(0, t) > d_1$. From Eqs. (20) and (23) it follows that

$$\alpha(t, d_1, d_2) = \int_0^t g(t', d_1, d_2)\,dt' \,. \quad (30)$$

Hence,

$$\alpha(t, d_1, d_2) = \alpha_i(t, d_1, d_2) + \alpha_s(t, d_1, d_2) \,, \quad (31)$$

where the first component of the conversion degree results from the spherulites nucleated inside a sample, while the second is related to spherulites nucleated at the sample boundaries:

$$\alpha_i(t, d_1, d_2) = \int_0^t g_i(t', d_1, d_2)\,dt' \quad (32)$$

$$\alpha_s(t, d_1, d_2) = \int_0^t g_s(t', d_1, d_2)\,dt' \quad (33)$$

From the above considerations it is evident that the conversion degree and also the rate of conversion of a sample into spherulites depend on distances to sample boundaries; they are different near sample surfaces and deep inside a sample.

The calculations of the average conversion degree within sample as well as the average rate of spherulite interiors formation involve integration over the range $0 < d_1 < 2h$ followed by dividing the result by $2h$. If spherulite growth rate and nucleation rate depend only on time we may limit integration to $0 < d_1 < h$ due to sample symmetry. The respective expressions will be given below for various relations of the sample thickness, $2h$, with respect to $r(0, t)$:

– *Range 1:* $h > r(0, t)$.

$$\alpha_{av}(t, 2h) = 1 - h^{-1}\exp[-E(t)]\{h - r(0, t) + \int_0^{r(0,t)} \exp[-H(t, s)]\,ds\} \,, \quad (34)$$

$$g_{iav}(t, 2h)\,dt = h^{-1}\exp[-E(t)]\{W(t)[h - r(0, t)] + \int_0^{r(0,t)} \exp[-H(t, s)][W(t) - R_i(t, s)]\,ds\} \,, \quad (35)$$

$$g_{sav}(t, 2h)\,dt = h^{-1}\exp[-E(t)] \times \left\{\int_0^{r(0,t)} \exp[-H(t, s)]\,R_s(t, s)\,ds\right\} \,. \quad (36)$$

– *Range 2:* $2h > r(0, t) > h$.

$$\alpha_{av}(t, 2h) = 1 - h^{-1}\exp[-E(t)]\left\{\int_0^{2h-r(0,t)} \exp[-H(t, s)]\,ds + \int_{2h-r(0,t)}^{h} \exp[-H(t, s) - H(t, d - s)]\,ds\right\} \,, \quad (37)$$

$$g_{iav}(t, 2h)\,dt = h^{-1}\exp[-E(t)] \times \left\{\int_0^{2h-r(0,t)} \exp[-H(t, s)]\,[W(t) - R_i(t, s)]\,ds + \int_{2h-r(0,t)}^{h} \exp[-H(t, s) - H(t, 2h - s)] \times [W(t) - R_i(t, s) - R_i(t, 2h - s)]\,ds\right\} \,, \quad (38)$$

$$g_{sav}(t, 2h)\,dt = h^{-1}\exp[-E(t)]\left\{\int_0^{2h-r(0,t)} \exp[-H(t,s)] \times R_s(t,s)\,ds + \int_{2h-r(0,t)}^{h} \exp[-H(t,s) - H(t,2h-s)] \times [R_s(t,s) + R_s(t,2h-s)\,ds\right\}. \quad (39)$$

– *Range 3:* $2h < r(0,t)$

$$\alpha_{av}(t, 2h) = 1 - h^{-1}\exp[-E(t)]\int_0^h \exp[-H(t,s) - H(t,2h-s)]\,ds\,, \quad (40)$$

$$g_{iav}(t, 2h)\,dt = h^{-1}\exp[-E(t)]\int_0^h \exp[-H(t,s) - H(t,2h-s)][W(t) - R_i(t,s) - R_i(t,2h-s)]\,ds\,, \quad (41)$$

$$g_{sav}(t, 2h)\,dt = h^{-1}\exp[-E(t)]\int_0^h \exp[-H(t,s) - H(t,2h-s)]\,[R_s(t,s) + R_s(t,2h-s)]\,ds\,. \quad (42)$$

It should be noted that for each range of relation between h and $r(0, t)$ the following relationships are fulfilled:

$$g_{av}(t, 2h) = g_{iav}(t, 2h) + g_{sav}(t, 2h)\,, \quad (43)$$

$$\alpha_{iav}(t, 2h) = \int_0^t g_{iav}(t', 2h)\,dt'\,, \quad (44)$$

$$\alpha_{sav}(t, 2h) = \int_0^t g_{sav}(t', 2h)\,dt'\,, \quad (45)$$

$\alpha_{sav}(t, 2h)$ multiplied by h is the average thickness of a layer at time t of spherulites nucleated at sample boundary. $\alpha_{iav}(\infty, 2h)$ and $\alpha_{sav}(\infty, 2h)$ represent the fractions of sample occupied after completion of crystallization by those spherulites which were nucleated inside a sample and at sample boundaries, respectively.

It follows from Eqs. (34)–(42) that the process of spherulitic structure formation depends not only on the nucleation rate and the spherulite growth rate but also on the sample thickness. Depending on the relation of value of $r(0, t)$ at the end of crystallization and sample thickness, $2h$, one has to consider only the range 1, the ranges 1 and 2 or all three ranges: 1,2 and 3. It should be noted here that for G = const. formulas (34), (37) and (40) describing the average conversion degree become identical to those derived by Billon et al. [4] for isothermal crystallization. No comparable data are found in the literature for the relationships describing the contributions from spherulites nucleated at sample boundaries and inside a sample to the conversion degree and to the conversion rate.

The number of spherulites, $N_i\,dt$, nucleated at the distances d_1 and d_2 from sample boundaries and the average number of spherulites, $N_{iav}\,dt$, nucleated in time interval $(t, t + dt)$ in unit area (or volume) of the sample are expressed as follows:

$$N_i(t, d_1, d_2)\,dt = F(t)\,dt[1 - \alpha(t, d_1, d_2)]\,, \quad (46a)$$

$$N_{iav}(t, 2h)\,dt = F(t)\,dt\,[1 - \alpha_{av}(t, 2h)]\,. \quad (46b)$$

The number of spherulites nucleated at sample boundaries in time interval $(t, t + dt)$ per unit length or area of boundary is expressed by the formula:

$$N_s(t)\,dt = F_s(t)\,dt\,[1 - \alpha(t, 0, 2h)]\,. \quad (47)$$

To calculate the respective numbers of spherulites nucleated during the time interval t, one has to integrate the expressions (46)–(47) over the range $0 < t' < t$. For $t \to \infty$ the respective numbers of spherulites after completion of crystallization are obtained.

It follows from the above considerations that sample boundaries influence the formation of spherulitic structure within a distance equal to $r(0, t)$. The conversion degree time dependence and time dependencies of the formation of spherulite interiors differ from those for infinite samples. It follows from Eqs. (34) and (35) that the influence of sample boundaries can be neglected only if the sample thickness $2h$ is much greater than $2r(0, t)$ because then $\alpha_{av}(t, 2h)$ and $g_{iav}(t, 2h)$ approaches $\alpha(t)$ and $g(t)$ for infinite samples. If there is no nucleation at sample boundaries the conversion degree in the vicinity of sample boundary is lower than in an infinite sample after the same time elapsed from the beginning of crystallization: at the boundary, for $r(0, t) < h$, the probability that the point is unoccluded equals the square root of the probability of the same event for infinite sample. For $r(0, t) > 2h$ the delay in crystallization at sample boundary is even stronger since the conversion degree there is influenced also by the opposing boundary surface. In absence of spherulite nucleation at boundaries the averaged conversion degree in strips and plates is always lower than in infinite samples at the same time. Slower conversion of melt into spherulites results also in a larger number of spherulites nucleated inside a sample (see Eqs. (46)) if nucleation process is extended in time.

Extended radius

Similarly, as for infinite samples [15] the substitution:

$$z = r(0, \tau) \quad \text{and} \quad R = r(0, t) \quad (48)$$

reduces the expressions for the time dependencies of conversion degree and spherulite interiors formation to

simpler forms:

$$\alpha_N(R, d_1, d_2) = 1 - \exp[- E_N(R) - H_N(R, d_1) - H_N(R, d_2)] , \quad (49)$$

$$g_N(R, d_1, d_2)dR = \exp[- E_N(R) - H_N(R, d_1) - H_N(R, d_2)][W_N(R) + W_{N1}(R, d_1) + W_{N1}(R, d_2)] , \quad (50)$$

where

$$E_N(R) = v\pi \int_0^R P(z)(R - z)^k \, dz \quad (51)$$

with $v = 1$, $k = 2$ for 2D case and $v = \frac{4}{3}$, $k = 3$ for 3D case,

$$W_N(R) = \frac{dE_N(R)}{dR} dR ; \quad (52)$$

For $R < d$:

$$H_N(R, d) = 0 \quad \text{and} \quad W_{N1}(R, d) = 0 ; \quad (53)$$

For $R > d$:

$$H_N^{(2)}(R, d) = \int_0^{R-d} \Big\{ 2P_s(z)[(R - z)^2 - d^2]^{0.5} - P(z)\{(R - z)^2 \gamma(d,(R - z)) - d[(R - z)^2 - d^2]^{0.5}\} \Big\} dz ; \quad (54a)$$

$$H_N^{(3)}(R, d) = \pi \int_0^{R-d} \{P_s(z)[(R - z)^2 - d^2] - P(z)[2(R - z)^3 - d^3 - 3d(R - z)^2]/3\} dz ; \quad (54b)$$

$$W_{N1}(R, d) = \frac{\partial H_N(R, d)}{\partial R} dR , \quad (55)$$

where γ is given by Eq. (15), $P(z) = F_N(z)/G_N(z)$, $P_s(z) = F_{sN}(z)/G_N(z)$, $F_{sN}(z) = F_s(\tau)$, $F_N(z) = F(\tau)$ and $G_N(z) = G(\tau)$.

In a similar way one can express also the time distributions of the formation of spherulites interiors separately for spherulites nucleated inside a sample and for spherulites nucleated at sample boundaries.

It follows that the local kinetics of spherulites structure formation expressed in terms of $R(t)$ depends on the distances from sample boundaries and on the dependencies of the ratios: $F(t)/G(t)$ and $F_s(t)/G(t)$ on $R(t)$. Averaged dependencies across the sample thickness depend on the sample thickness instead of the distances from sample boundaries.

Distributions of distances from spherulite centers to spherulite inner points

Equation (13) permits us to derive the expression for the probability that the spherulite nucleated at time τ occludes an arbitrary point A in the distance r from its center:

$$p_{T*}(r, \tau) = \exp[- E_T(t(r, \tau), d_1, d_2)] \Delta V_T(\tau, t(r, \tau)) d\tau , \quad (56)$$

where E_T and ΔV_T are given by Eqs. (21) and (19b), $t(r, \tau)$ denotes the time of occlusion of the point A, dependent on distance r and on nucleation time of a spherulite τ:

$$\int_0^t G(s) \, ds = r + \int_0^\tau G(s) \, ds . \quad (57)$$

The integration of $p_{T*}(r, \tau)$ over the range $0 < \tau < \infty$ results in the distribution of distances from spherulite centers to spherulite inner points, $f(r, d_1, d_2) dr$. Substitution of Eq. (48) permits to write $f(r, d_1, d_2) dr$ in the simpler form:

$$f(r, d_1, d_2) dr = f_i(r, d_1, d_2) dr + f_s(r, d_1, d_2) dr , \quad (58)$$

where

$$f_i(r, d_1, d_2) dr = [\Delta V^*(r) - \Delta S^*(r, d_1) - \Delta S^*(r, d_2)] \times \int_0^\infty P(z) \exp[- E_N(r + z) - H_N(r + z, d_1) - H_N(r + z, d_2)] dz , \quad (59)$$

$$f_s(r, d_1, d_2) dr = [\Delta L^*(r, d_1) + \Delta L^*(r, d_2)] \times \int_0^\infty P_s(z) \exp[- E_N(r + z) - H_N(r + z, d_1) - H_N(r + z, d_2)] dz , \quad (60)$$

$\Delta V^*(r)$, $\Delta S^*(r, d)$ and $\Delta L^*(r, d)$ are readily obtained from $\Delta V(\tau, t)$, $\Delta S(\tau, t, d)$ and $\Delta L(\tau, t, d)$ by substitution $r(\tau, t) = r$. $f(r, d_1, d_2) dr$ represents a fraction of a sample in the distance $(r, r + dr)$ from spherulites centers. The two components f_i and f_s describe the distributions of distances for spherulites nucleated inside a sample and for spherulites nucleated at sample surfaces, respectively. For $r < d$, $\Delta S^*(r, d)$ and $\Delta L^*(r, d)$ are zero, hence for the respective ranges of r the distributions of distances are expressed as follows:

1. $r < d_1 < d_2$:

$$f_{i1}(r, d_1, d_2) dr = \Delta V^*(r) B(r, d_1, d_2) , \quad (61)$$

$$f_{s1}(r, d_1, d_2) dr = 0 . \quad (62)$$

2. $d_2 > r > d_1$:

$$f_{i2}(r, d_1, d_2)\,dr = [\Delta V^*(r) - \Delta S^*(r, d_1)]\,B(r, d_1, d_2)\,, \quad (63)$$

$$f_{s2}(r, d_1, d_2)\,dr = \Delta L^*(r, d_1)\,C(r, d_1, d_2)\,. \quad (64)$$

3. $r > d_2 > d_1$:

$$f_{i3}(r, d_1, d_2)\,dr = [\Delta V^*(r) - \Delta S^*(r, d_1) - \Delta S^*(r, d_2)]\,B(r, d_1, d_2)\,, \quad (65)$$

$$f_{s3}(r, d_1, d_2)\,dr = [\Delta L^*(r, d_1) + \Delta L^*(r, d_2)]\,C(r, d_1, d_2)\,, \quad (66)$$

where

$$B(r, d_1, d_2) = \int_0^\infty P(z)\exp[-E_N(r+z) - H_N(r+z, d_1) - H_N(r+z, d_2)]\,dz\,, \quad (67)$$

$$C(r, d_1, d_2) = \int_0^\infty P_s(z)\exp[-E_N(r+z) - H_N(r+z, d_1) - H_N(r+z, d_2)]\,dz \quad (68)$$

and $H_N(r+z, d) = 0$ for $z < d - r$.

In order to calculate the averaged distance distributions across the sample thickness one has to integrate expressions (61)–(66) over the appropriate ranges of distances from a sample boundary. Hence, for $r < h$:

$$f_{av}(r, 2h)\,dr = h^{-1}\left[\int_r^h f_1(r, s, 2h-s)\,ds + \int_0^r f_2(r, s, 2h-s)\,ds\right] dr \quad (69)$$

– for $2h > r > h$;

$$f_{av}(r, 2h)\,dr = h^{-1}\left[\int_0^{2h-r} f_2(r, s, 2h-s)\,ds + \int_{2h-r}^h f_3(r, s, 2h-s)\,ds\right] dr \quad (70)$$

– for $r > 2h$:

$$f_{av}(r, 2h)\,dr = h^{-1}\int_0^h f_3(r, s, 2h-s)\,ds\,dr\,. \quad (71)$$

Equations (69)–(71) are valid for the distance distribution f as well as for both its components f_i and f_s. It follows from the above relationships that the spherulitic structure formed in samples of finite thickness is fully determined by the ratios of nucleation rates to spherulite growth rate, P and P_s, if expressed as a function of $R(t)$, and by the distances to sample boundaries. The averaged distributions of distances depend on P and P_s and on the sample thickness, $2h$. It should be noted that in all cases considered the distributions of distances from the spherulite centers to their inner points differ from respective distributions of distances for infinite samples. The weakest influence of sample boundaries is in the case when $r < h$ and is the strongest when $r > 2h$. The distributions of distances tend to zero for $r \to \infty$. Nevertheless, the time t for which conversion degree approaches 1, sets the upper limit equal to $r(0, t)$ for the distance, r, between centers of spherulites and portions of those spherulites in real samples. Hence, if the sample thickness, $2h$, is much greater than $2r(0, t)$ at the end of crystallization, the distributions of distances approach those for infinite samples.

It should be noted that the integration of f_i and f_s over the range $0 < r < \infty$ permits to obtain a fraction of a sample occupied after completion of crystallization by spherulites nucleated inside a sample and by spherulites nucleated at sample boundaries.

Semiinfinite samples

In a semiinfinite sample only one sample boundary influences the formation of spherulitic structure. According to Eqs. (20)–(26) one can express the conversion degree and the rate of formation of spherulite interiors, g, at the distance d_1 from a sample boundary, as follows:

$$\alpha(t, d_1) = 1 - \exp[-E(t) - H(t, d_1)]\,, \quad (72a)$$

$$g(t, d_1)\,dt = \exp[-E(t) - H(t, d_1)]\,[W(t) + W_1(t, d_1)]\,, \quad (72b)$$

where E, H, W and W_1 are defined by Eqs. (5), (6), (22), (24)–(26). H and W_1 are zero functions for $d_1 > r(0, t)$. The distributions of distances are in the form:

$$f(r, d_1)\,dr = [\Delta V^*(r) - \Delta S^*(r, d_1)]\int_0^\infty P(z)\exp[-E_N(r+z) - H_N(r+z, d_1)]\,dz + \Delta L^*(r, d_1) \times \int_0^\infty P_s(z)\exp[-E_N(r+z) - H_N(r+z, d_1)]\,dz\,, \quad (73)$$

where: $\Delta S^*(r, d_1) = 0$ and $\Delta L^*(r, d_1) = 0$ for $r < d_1$, $H_N(r+z, d_1) = 0$ for $r + z < d_1$ which results in different forms of $f(r, d_1)\,dr$ for $r < d_1$ and for $r > d_1$. The average values of α, g, and f, over a certain distance from a sample boundary are obtained by respective integration.

Thin samples

Let us assume that the sample is so thin that $r(0, t)$ becomes much greater than the sample thickness, $2h = \Delta h$,

Colloid & Polymer Science, Vol. 275, No. 11 (1997)

shortly after the beginning of crystallization process: $r(0, t) \gg \Delta h$. Then, the times t_1 and t_2, for which $r(t_1, t) = d_1$ and $r(t_2, t) = d_2$, are close to t, so circles and spheres of radius $r(\tau, t)$ turn into strips and disks of the thickness Δh. If we denote: $F^*(\tau) = F(\tau)\Delta h + 2F_s(\tau)$, the expressions for the conversion degree and the rate of formation of spherulite interiors are in the following forms:

$$\alpha(t, \Delta h) = 1 - \exp[-E(t, \Delta h)] , \tag{74}$$

$$g(t, \Delta h)\,dt = \exp[-E(t, \Delta h)]\,[W(t, \Delta h)] , \tag{75}$$

where

$$E^{(2)}(t, \Delta h) = 2\int_0^t F^*(\tau)\, r(\tau, t)\, d\tau , \tag{76a}$$

$$W^{(2)}(t, \Delta h) = 2\int_0^t F^*(\tau)\, d\tau\, G(t)\, dt , \tag{76b}$$

$$E^{(3)}(t, \Delta h) = \pi\int_0^t F^*(\tau)\, r^2(\tau, t)\, d\tau , \tag{77a}$$

$$W^{(3)}(t, \Delta h) = 2\pi\int_0^t F^*(\tau)\, r(\tau, t)\, d\tau\, G(t)\, dt . \tag{77b}$$

The distributions of distances from spherulite centers to spherulites inner points are expressed by the formulas:

$$f^{(2)}(r, \Delta h)\,dr = 2\int_0^\infty F^*(\tau)\exp[-E^{(2)}(t(r, \tau), \Delta h)]\,d\tau\,dr , \tag{78a}$$

$$f^{(3)}(r, \Delta h)\,dr = 2\pi r\int_0^\infty F^*(\tau)\exp[-E^{(3)}(t(r, \tau), \Delta h)]\,d\tau\,dr . \tag{78b}$$

Equations (74)–(76) and (78a) describe the spherulitic structure formation and its final pattern in infinite 1D sample – on a line, while Eqs. (74), (75), (77) and (78b) – in infinite 2D sample [14–16]. Hence, if spherulite extended radius is much greater than the sample thickness the dimensionality of the crystallization process decreases.

Conclusions

It was demonstrated that the probabilistic approach based on the concept of nucleation process as randomly fluctuated in space and in time can be successfully applied to the description of isothermal as well as nonisothermal crystallization in samples of finite thickness. Crystallization in semiinfinite samples was also considered. It is possible to obtain the conversion degree as a function of time and the respective expressions for the isothermal crystallization are identical to those obtained from Avrami and Evans theory by Billon et al. [4] and Escleine et al. [18]. The presented approach makes possible to describe the formation of spherulitic structures during the course of crystallization by means of the rates of formation of spherulites interiors and to differentiate spherulites nucleated inside a sample and at a sample boundaries. This permits to evaluate the contributions of both spherulite populations to the conversion degree during the crystallization process. It is also possible to describe the final spherulitic pattern by means of distributions of distances from spherulite centers to their inner points.

It was demonstrated that the presence of sample boundaries influences the crystallization process within a distance equal to spherulite extended radius (the integral of spherulitic growth rate calculated from the beginning of crystallization). The distribution of distances from spherulites centers to inner points of those spherulites is also afflicted by sample boundaries. It was shown that the sample can be treated as infinite only if the extended radius at the end of crystallization process is much smaller than half of the sample thickness. In contrast, a thin film can be treated as two-dimensional only when the extended radius is much greater than the sample thickness. In the absence of additional nucleation at sample boundaries the process of structure formation within a distance equal to the extended radius from the boundary is slower than for infinite samples. If the influence of the opposite boundary can be neglected, the conversion degree at the sample boundary can be expressed as $1 - [1 - \alpha_{if}(t)]^q$ with $q = \frac{1}{2}$ where $\alpha_{if}(t)$ denotes the conversion degree of an infinite sample. It is easy to notice that at a corner of thin film and on an edge of bulk sample where two perpendicular boundaries meet q equals $\frac{1}{4}$, while at corners of bulk samples q equals $\frac{1}{8}$. Therefore, much slower structure formation in such areas could be expected. Hence, if primary nucleation is prolonged in time a larger number of spherulites will be nucleated. However, during crystallization of real samples those effects can be masked by the temperature gradient across a sample due to cooling and/or by nucleation at sample boundaries. The spherulites originating from surface nuclei grow on the account of those originating in the interior of the material. They speed up the conversion within a distance equal to spherulite extended radius. The effect appears even for weak intensity of nucleation at sample boundaries but increases with increasing intensity. The nucleation at sample boundaries influences also the final spherulitic pattern. In the above consideration only the flat parallel sample boundaries were considered although the present approach can be easily extended for the description of samples of any

shape. One can expect, however, that curvature of sample boundary can be significant only if its radius is of the order of the extended spherulite radius at the respective moment of time.

Acknowledgement This research was supported primarily by the State Committee for Scientific Research, Poland, through the Centre of Molecular and Macromolecular Studies, PAS, under Grant 2 P303 101 04.

References

1. Kolmogoroff AN (1937) Izvestiya Akad Nauk SSSR, Ser Math 1:355
2. Evans UR (1945) Trans Faraday Soc 41:365
3. Avrami M (1939) J Chem Phys 7:1103, (1939) ibid 8:212, (1940) ibid 9:177
4. Billon N, Escleine JM, Haudin JM (1989) Colloid Polym Sci 267:668
5. Ozawa T (1971) Polymer 12:150
6. Galeski A (1981) J Polym Sci, Polym Phys Ed 19:721
7. Galeski A, Piorkowska E (1981) J Polym Sci, Polym Phys Ed 19:731
8. Hay JN, Przekop ZJ (1979) J Polym Sci, Polym Phys Ed 17:951
9. Hay JN, Booth A (1972) Br Polym J 4:19
10. Price FP (1969) J Appl Phys 36:3014
11. Grenier D, Prudhomme RE (1980) J Polym Sci, Polym Phys Ed 18:1655
12. Piorkowska E, Galeski A (1985) J Phys Chem 89:4700
13. Piorkowska E, Galeski A (1985) J Polym Sci, Polym Phys Ed 23:1273
14. Piorkowska E (1995) J Chem Phys 99: 14007
15. Piorkowska E (1995) J Chem Phys 99: 14016
16. Piorkowska E (1995) J Chem Phys 99: 14024
17. Galeski A, Piorkowska E (1983) Colloid Polym Sci 261:1
18. Escleine JM, Monasse B, Wey E, Haudin JM (1984) Colloid Polym Sci 262:366
19. Billon N and Haudin JM (1989) Ann Chim Fr 15:249
20. Billon N and Haudin JM (1989) Colloid Polym Sci 267:1064
21. Billon N, Magnet C, Haudin JM and Lefebvre D (1994) Colloid Polym Sci 272:633
22. Piorkowska E, Galeski A (1994) Polimery 39:502
23. Mehl NA, Rebenfeld L (1993) J Polym Sci, Part B, Polym Phys 31:1677
24. Mehl NA, Rebenfeld L (1993) J Polym Sci, Part B, Polym Phys 31:1687
25. Krause T, Kalinka G, Auer C, Hindrichsen G (1994) J Appl Polym Sci 51:399
26. Auer C, Kalinka G, Krause T, Hindrichsen G (1994) J Appl Polym Sci 51:413